Short Note

6-Chloro-3-nitro-8-(phenylthio)-2-[(phenylthio)methyl]imidazo[1,2-*a*]pyridine

Romain Paoli-Lombardo [1]**, Nicolas Primas** [1,2,]*****, Sébastien Hutter** [3]**, Sandra Bourgeade-Delmas** [4]**, Clotilde Boudot** [5]**, Caroline Castera-Ducros** [1,2]**, Inès Jacquet** [1]**, Bertrand Courtioux** [5]**, Nadine Azas** [3]**, Pascal Rathelot** [1,2] **and Patrice Vanelle** [1,2,]*****

[1] CNRS, ICR UMR 7273, Team Pharmaco-Chimie Radicalaire, Faculté de Pharmacie, Aix Marseille University, 27 Boulevard Jean Moulin, CS30064, CEDEX 05, 13385 Marseille, France; romain.paoli-romain.paoli-lombardo@etu.univ-amu.fr (R.P.-L.); caroline.ducros@univ-amu.fr (C.C.-D.); ines.jacquet@etu.univ-amu.fr (I.J.); pascal.rathelot@univ-amu.fr (P.R.)

[2] AP-HM, Service Central de la Qualité et de l'Information Pharmaceutiques, Hôpital de la Conception, 13005 Marseille, France

[3] IHU Méditerranée Infection, UMR VITROME-Tropical Eukaryotic Pathogens, Aix Marseille University, 19–21 Boulevard Jean Moulin, 13005 Marseille, France; sebastien.hutter@univ-amu.fr (S.H.); nadine.azas@univ-amu.fr (N.A.)

[4] UMR 152 PHARMA-DEV, University of Toulouse, IRD, 31062 Toulouse, France; sandra.bourgeade-delmas@ird.fr

[5] UMR Inserm 1094, Neuroépidémiologie Tropicale, Faculté de Pharmacie, University of Limoges, 2 Rue Du Dr Marcland, 87025 Limoges, France; bertrand.courtioux@unilim.fr (B.C.)

***** Correspondence: nicolas.primas@univ-amu.fr (N.P.); patrice.vanelle@univ-amu.fr (P.V.)

Abstract: As part of our ongoing antikinetoplastid structure–activity relationship study focused on positions 2 and 8 of the 3-nitroimidazo[1,2-*a*]pyridine scaffold, we were able to introduce a phenylthioether moiety at both position 2 and position 8 in one step. Using a previously reported synthetic route developed in our laboratory, we obtained 6-chloro-3-nitro-8-(phenylthio)-2-[(phenylthio)methyl]imidazo[1,2-*a*]pyridine in 74% yield. The in vitro cell viability of this compound was assessed on the HepG2 cell line, and its in vitro activity was evaluated against the promastigote form of *L. donovani*, the axenic amastigote form of *L. infantum* and the trypomastigote blood stream form of *T. b. brucei*. It showed low solubility in HepG2 culture medium ($CC_{50} > 7.8$ μM), associated with weak activity against both the promastigote form of *L. donovani* ($EC_{50} = 8.8$ μM), the axenic amastigote form of *L. infantum* ($EC_{50} = 9.7$ μM) and the trypomastigote blood stream form of *T. b. brucei* ($EC_{50} = 12.8$ μM).

Keywords: imidazo [1,2-*a*] pyridine; nitroaromatic; structure–activity relationship; *Leishmania* spp.; *Trypanosoma brucei*

1. Introduction

In humans, kinetoplastid diseases are caused by flagellated protozoa of the genus *Leishmania* and *Trypanosoma* [1]. Leishmaniases (*Leishmania* spp.) and sleeping sickness (*Trypanosoma brucei*) are defined by the World Health Organization (WHO) as neglected tropical diseases (NTDs), mainly present in developing countries [2]. Threatening more than one billion people worldwide, these two diseases are responsible for nearly 50,000 deaths per year [3,4].

Among the twenty species of *Leishmania* responsible for infection in people, two are responsible for life-threatening visceral leishmaniasis (VL): *L. donovani* in Asia and Africa, and *L. infantum* in the Mediterranean Basin and Latin America [5]. Between 50,000 and 90,000 new cases and more than 30,000 deaths due to VL are reported annually [6]. For sleeping sickness, about 60 million people in 36 sub-Saharan African countries are considered to be at risk of contracting it [7]. Since 2019, less than 1000 cases are recorded

by the WHO annually, but this number is probably underestimated because of the under-diagnosis of the disease [8]. In the absence of a vaccine [9], VL and sleeping sickness are treated with a small spectrum of very few efficient, safe and affordable drugs [10].

As part of our research program to develop new potential antikinetoplastid derivatives in the 3-nitroimidazo[1,2-*a*]pyridine series, our team previously described a hit molecule (Hit A), bearing a phenylsulfonylmethyl substituent at position 2; a chlorine atom at position 6 and a 4-chlorophenylthioether moiety at position 8 (Table 1) [11]. Its influence on cell viability (cytotoxic concentration 50% = CC_{50}) was assessed on the human hepatocyte HepG2 cell line, showing low cytotoxicity. In vitro activities (measured by the effective concentration 50% = EC_{50}) were evaluated against both the promastigote form of *L. donovani*, the axenic amastigote form of *L. infantum* and the trypomastigote bloodstream form (BSF) of *T. b. brucei*. Hit A displayed micromolar activities on all these forms.

Table 1. Structures and biological profiles of previously identified Hit A and Molecule B.

|	Hit A	Molecule B
EC_{50} *L. donovani* promastigotes (μM)	1.0 ± 0.3	7.4 ± 0.4
EC_{50} *L. infantum* axenic amastigotes (μM)	1.7 ± 0.3	-
EC_{50} *T. b. brucei* BSF (μM)	0.95 ± 0.05	>50
CC_{50} HepG2 (μM)	>100	>15.6

After identifying this hit compound, a phenylthiomethyl analogue (Molecule **B**) was obtained and evaluated in vitro (Table 1) [12]. Replacement of the sulfone with a sulfur atom resulted in decreased solubility in HepG2 culture medium and decreased antileishmanial activity, as well as a loss of antitrypanosomal activity.

Throughout our structure–activity relationship study focused on positions 2 and 8 of the 3-nitroimidazo[1,2-*a*]pyridine scaffold; we were able to introduce a phenylthioether moiety at both position 2 and position 8. This allowed us to replace the sulfone at position 2 with a sulfur atom and remove the chlorine atom at the para position of the phenyl ring at position 8, using a single reaction.

2. Results and Discussion

2.1. Synthesis

Using a previously described synthetic route developed in our laboratory [13], 3-bromo-5-chloropyridin-2-amine was cyclized into the corresponding 2-chloromethylimidazo[1,2-*a*]pyridine intermediate 1 by reaction with 1,3-dichloroacetone in refluxing ethanol, followed by a selective nitration reaction at the position 3, giving 3-nitroimidazo[1,2-*a*]pyridine derivative 2 (Scheme 1).
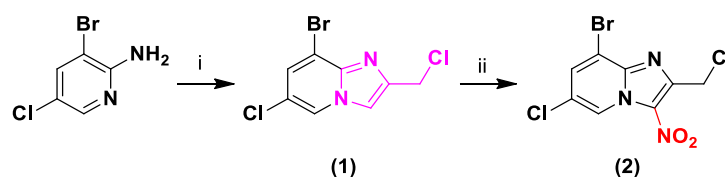
Scheme 1. Synthesis of compounds (**1**) and (**2**).

Reagents and conditions: (i) 1,3-Dichloroacetone 1.1 equiv, EtOH, reflux, 96 h, 60%; (ii) HNO_3 65% 6 equiv, H_2SO_4, 0 °C→RT, 3 h, 60%.

Then, compound 3 was obtained in good yield by substituting both the chlorine atom of the chloromethyl group at position 2 and the bromine atom at position 8 of substrate 2 with sodium thiophenolate formed in situ with NaH in DMSO at room temperature (Scheme 2).
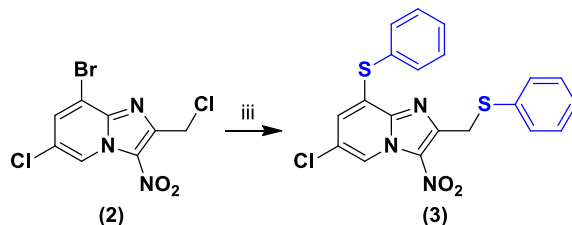
Scheme 2. Synthesis of compound (**3**).

Reagents and conditions: (3) Thiophenol 2 equiv, NaH 60% 2 equiv, DMSO, N_2, RT, 15 h, 74%.

2.2. Biological Results

The cell viability of compound 3 was assessed on the HepG2 cell line, and doxorubicin was used as a positive control. The antileishmanial activity was evaluated in vitro against both the promastigote form of *L. donovani* and the axenic amastigote form of *L. infantum*. The antitrypanosomal activity was determined on the trypomastigote bloodstream form of *T. b. brucei*. Biological profiles were compared to Hit A, Molecule B and reference drugs (amphotericin B, miltefosine, fexinidazole and suramin) (Table 2 and Table S1).

Table 2. In vitro evaluation of molecule 3 on the human hepatocyte HepG2 cell line, *L. donovani* promastigotes, *L. infantum* axenic amastigotes and *T. b. brucei* trypomastigotes BSF.

	CC_{50} HepG2 (μM)	EC_{50} *L. Dono.* Pro. (μM)	EC_{50} *L. Inf.* Axenic Ama. (μM)	EC_{50} *T. B. Brucei* BSF (μM)
3	>7.8 [a]	8.8 ± 1.5	9.7 ± 1.2	12.8 ± 0.8

[a] The product could not be tested at higher concentrations due to a lack of solubility in the culture medium.

Compared to Hit A, compound 3 showed low solubility in HepG2 culture medium (CC_{50} > 7.8 μM), associated with decreased activity against both the promastigote form of *L. donovani* (EC_{50} = 8.8 μM), the axenic amastigote form of *L. infantum* (EC_{50} = 9.7 μM) and the trypomastigote bloodstream form of *T. b. brucei* (EC_{50} = 12.8 μM). However, compound **3** displayed similar antileishmanial activity and showed a better antitrypanosomal EC_{50} value than Molecule **B** (EC_{50} = 7.4 μM and EC_{50} > 50 μM, respectively).

Thus, the replacement of the sulfone at position 2 with a sulfur atom, leading to Molecule B and compound 3, resulted in both a loss of solubility and a decrease in antileishmanial and antitrypanosomal activity. However, the chlorine atom at the para position of the phenyl ring at position 8 did not appear to be essential to the activity and even led to a slight improvement in antitrypanosomal activity.

3. Materials and Methods

3.1. Chemistry

3.1.1. General

Melting points were determined on a Köfler melting point apparatus (Wagner & Munz GmbH, München, Germany) and were uncorrected. The infrared (IR) spectrum was measured for pure products on a Bruker VERTEX70 FTIR spectrometer equipped with a Bruker A222 Attenuated Total Reflection (ATR) accessory at the Faculté des Sciences de Saint-Jérôme (Marseille). The crystal used is a diamond. The spectrometer is equipped with a Globar source and a KBr/DLaTGS detector. Each spectrum is recorded with 30 scans and a scanning speed of 10 KHz in the spectral range of 4000–400 cm^{-1}. The apodization

function used is Blackman-Harris 3 terms. The spectrometer is continuously purged with dry CO_2-free air. The spectrum of the ATR accessory without a sample served as a reference. The temperature inside the spectrometer has been kept constant at 25 °C. UV–Vis absorption spectra were recorded at the Faculté des Sciences de Saint-Jérôme (Marseille) with a Jasco V670 instrument equipped with a Peltier cell holder ETCS-761 to maintain the temperature at 20.0 °C. A quartz cell of 1 mm of optical path length was used. Solution of compound 3 with a concentration of 0.16 g.L^{-1} was prepared in acetonitrile (HPLC grade). The UV-vis absorption spectra were recorded using the solvent as a reference and are presented without smoothing and further data processing. The measurement range was 200–800 nm with a data interval of 2 nm, a scan speed of 400 nm/min and a UV-vis bandwidth of 2 nm. HRMS spectrum (ESI) was recorded on a SYNAPT G2 HDMS (Waters) at the Faculté des Sciences de Saint-Jérôme (Marseille). NMR spectra were recorded on a Bruker Avance 200 MHz or a Bruker Avance NEO 400 MHz NanoBay spectrometer at the Faculté de Pharmacie of Marseille. (^{1}H NMR: reference CDCl$_3$ δ = 7.26 ppm, reference DMSO-d_6 δ = 2.50 ppm and ^{13}C NMR: reference CDCl$_3$ δ = 76.9 ppm, reference DMSO-d_6 δ = 39.52 ppm). The following adsorbent was used for column chromatography: silica gel 60 (Merck KGaA, Darmstadt, Germany, particle size 0.063–0.200 mm, 70–230 mesh ASTM). TLC was performed on 5 cm x 10 cm aluminum plates coated with silica gel 60F-254 (Merck) in an appropriate eluent. Visualization was performed with ultraviolet light (234 nm). The purity determination of synthesized compounds was checked by LC/MS analyses, which were realized at the Faculté de Pharmacie of Marseille with a Thermo Scientific Accela High-Speed LC System® (Waltham, MA, USA) coupled using a single quadrupole mass spectrometer Thermo MSQ Plus®. The purity of synthesized compound **3** was > 95%. The RP-HPLC column is a Thermo Hypersil Gold® 50 × 2.1 mm (C$_{18}$ bounded), with particles of a diameter of 1.9 mm. The volume of the sample injected into the column was 1 μL. Chromatographic analysis, total duration of 8 min, was on the gradient of the following solvents: t = 0 min, methanol/water 50:50; 0 < t < 4 min, linear increase in the proportion of methanol to a methanol/water ratio of 95:5; 4 < t < 6 min, methanol/water 95:5; 6 < t < 7 min, linear decrease in the proportion of methanol to return to a methanol/water ratio of 50:50; 6 < t < 7 min, methanol/water 50:50. The water used was buffered with ammonium acetate 5 mM. The flow rate of the mobile phase was 0.3 mL/min. The retention times (tR) of the molecules analyzed were indicated in min. Reagents were purchased from Sigma-Aldrich or Fluorochem and used without further purification. Copies of ^{1}H NMR, ^{13}C NMR, IR and UV–Vis spectra are available in the Supplementary Materials.

3.1.2. 8-Bromo-6-chloro-2-chloromethylimidazo[1,2-*a*]pyridine (**1**)

To a solution of 3-bromo-5-chloropyridin-2-amine (5 g, 24.1 mmol, 1 equiv) in ethanol (80 mL), 1,3-dichloroacetone (3.34 g, 26.5 mmol, 1.1 equiv) was added. The reaction mixture was stirred and heated under reflux for 96 h. The solvent was then evaporated in vacuo. Compound 1 was obtained after purification by chromatography on silica gel (dichloromethane) as a yellow solid in 60% yield (4.1 g). mp 161 °C. ^{1}H NMR (200 MHz, CDCl$_3$) δ: 8.13 (d, *J* = 1.6 Hz, 1H), 7.71 (s, 1H), 7.48 (d, *J* = 1.6 Hz, 1H), 4.79 (s, 2H). ^{13}C NMR (50 MHz, CDCl$_3$) δ: 142.0, 137.7, 125.4, 122.4, 120.1, 116.0, 113.0, 39.1. LC/MS ESI + t$_R$ 1.77 min, (*m/z*) [M + H]$^+$ 278.80/280.85/282.84. HRMS (+ESI): 280.9064 [M + H]$^+$. Calcd for C$_8$H$_6$BrCl$_2$N$_2$: 280.9062.

3.1.3. 8-Bromo-6-chloro-2-chloromethyl-3-nitroimidazo[1,2-*a*]pyridine (**2**)

To a solution of 8-bromo-6-chloro-2-chloromethylimidazo[1,2-*a*]pyridine (1) (2 g, 7.2 mmol, 1 equiv) in concentrated sulfuric acid (20 mL) cooled by an ice-water bath, nitric acid 65% (1.9 mL, 43.2 mmol, 6 equiv) was added while keeping the temperature below 0 °C. The reaction mixture was stirred for 3 h at room temperature. Then, the mixture was slowly poured into an ice-water mixture and the desired product precipitated. Compound 2 was obtained after purification by chromatography on silica gel (eluent: dichloromethane)

as a yellow solid in 60% yield (1.4 g). mp 165 °C. ^{1}H NMR (200 MHz, CDCl$_3$) δ: 9.48 (d, J = 1.8 Hz, 1H), 7.92 (d, J = 1.8 Hz, 1H), 5.08 (s, 2H). ^{13}C NMR (50 MHz, CDCl$_3$) δ: 147.7, 140.9, 134.07, 129.9, 125.2, 124.7, 113.2, 38.2. LC/MS ESI + t$_R$ 2.51 min, (m/z) [M + H]$^+$ 324.00/325.93. HRMS (+ESI): 323.8938 [M + H]$^+$. Calcd for C$_8$H$_5$BrCl$_2$N$_3$O$_2$: 323.8937.

3.1.4. 6-Chloro-3-nitro-8-(phenylthio)-2-[(phenylthio)methyl]imidazo[1,2-*a*]pyridine (**3**)

To a sealed 20 mL flask containing sodium hydride (60% dispersion in mineral oil) (0.098 g, 2.46 mmol, 2 equiv) in dimethylsulfoxide (3 mL), thiophenol (253 μL, 2.46 mmol, 2 equiv) was added under N$_2$ atmosphere. The reaction mixture was stirred at room temperature for 30 min. Then, a solution of 8-bromo-6-chloro-2-chloromethyl-3-nitroimidazo [1,2-*a*]pyridine (2) (0.4 g, 1.23 mmol, 1 equiv) in dimethylsulfoxide (6 mL) was injected. The reaction mixture was stirred for 15 h at room temperature. The mixture was slowly poured into an ice-water mixture and precipitated. The solid was collected by filtration and dried under reduced pressure. Compound 3 was obtained after purification by chromatography on silica gel (eluent: cyclohexane-dichloromethane 5:5) as a yellow solid in 74% yield (0.36 g). mp 168 °C. IR (ATR) 3136, 3078, 3046, 3010, 2947, 2881, 2720, 2663, 1580, 1521, 1464, 1359, 1251, 1196, 1120, 809, 743, 690, 595, 476 cm^{-1}. UV-Vis (acetonitrile) λ$_{max}$ (ε$_{max}$, L.mol^{-1}.cm^{-1}) 382 (0.42), 296 (1.13), 250 (0.88), 220 (1.60) nm. ^{1}H NMR (400 MHz, DMSO-d_6) δ: 9.14 (d, J = 1.8 Hz, 1H), 7.69–7.62 (m, 2H), 7.62–7.55 (m, 3H), 7.46 (d, J = 7.4 Hz, 2H), 7.31 (t, J = 7.6 Hz, 2H), 7.27–7.19 (m, 1H), 6.83 (d, J = 1.8 Hz, 1H), 4.66 (s, 2H). ^{13}C NMR (100 MHz, DMSO-d_6) δ: 148.5, 139.5, 135.2, 134.7 (2C), 130.6, 130.5 (2C), 130.3, 129.4, 129.1 (2C), 130.0 (2C), 127.8, 126.5, 126.3, 123.5, 122.7, 32.0. LC/MS ESI + t$_R$ 5.25 min, (m/z) [M + H]$^+$ 427.84/429.71. HRMS (+ESI): 428.0286 [M + H]$^+$. Calcd for C$_{20}$H$_{15}$ClN$_3$O$_2$S$_2$: 428.0289.

References

1. Filardy, A.A.; Guimarães-Pinto, K.; Nunes, M.P.; Zukeram, K.; Fliess, L.; Pereira, L.; Nascimento, D.O.; Conde, L.; Morrot, A. Human Kinetoplastid Protozoan Infections: Where Are We Going Next? *Front. Immunol.* **2018**, *9*, 1493. [CrossRef] [PubMed]
2. Engels, D.; Zhou, X.-N. Neglected Tropical Diseases: An Effective Global Response to Local Poverty-Related Disease Priorities. *Infect. Dis. Poverty* **2020**, *9*, 10. [CrossRef] [PubMed]
3. World Health Organization (WHO). Leishmaniasis. Available online: https://www.who.int/news-room/fact-sheets/detail/leishmaniasis (accessed on 17 February 2023).
4. World Health Organization (WHO). Trypanosomiasis, Human African (Sleeping Sickness). 2020. Available online: https://www.who.int/news-room/fact-sheets/detail/trypanosomiasis-human-african-(sleeping-sickness) (accessed on 17 February 2023).
5. Burza, S.; Croft, S.L.; Boelaert, M. Leishmaniasis. *Lancet* **2018**, *392*, 951–970. [CrossRef] [PubMed]
6. Alvar, J.; Vélez, I.D.; Bern, C.; Herrero, M.; Desjeux, P.; Cano, J.; Jannin, J.; den Boer, M.; the Who Leishmaniasis Control Team. Leishmaniasis Worldwide and Global Estimates of Its Incidence. *PLoS ONE* **2012**, *7*, e35671. [CrossRef]

7.	Simarro, P.P.; Cecchi, G.; Franco, J.R.; Paone, M.; Diarra, A.; Ruiz-Postigo, J.A.; Fèvre, E.M.; Mattioli, R.C.; Jannin, J.G. Estimating and Mapping the Population at Risk of Sleeping Sickness. *PLoS Neglected Trop. Dis.* **2012**, *6*, e1859. [CrossRef] [PubMed]

8.	Mumba, D.; Bohorquez, E.; Messina, J.; Kande, V.; Taylor, S.M.; Tshefu, A.K.; Muwonga, J.; Kashamuka, M.M.; Emch, M.; Tidwell, R.; et al. Prevalence of Human African Trypanosomiasis in the Democratic Republic of the Congo. *PLoS Neglected Trop. Dis.* **2011**, *5*, e1246. [CrossRef] [PubMed]

9.	World Health Organization (WHO). Research Priorities for Chagas Disease, Human African Trypanosomiasis and Leishmaniasis. Available online: https://apps.who.int/iris/handle/10665/77472 (accessed on 17 February 2023).

10.	Kourbeli, V.; Chontzopoulou, E.; Moschovou, K.; Pavlos, D.; Mavromoustakos, T.; Papanastasiou, I.P. An Overview on Target-Based Drug Design against Kinetoplastid Protozoan Infections: Human African Trypanosomiasis, Chagas Disease and Leishmaniases. *Molecules* **2021**, *26*, 4629. [CrossRef] [PubMed]

11.	Fersing, C.; Basmaciyan, L.; Boudot, C.; Pedron, J.; Hutter, S.; Cohen, A.; Castera-Ducros, C.; Primas, N.; Laget, M.; Casanova, M.; et al. Nongenotoxic 3-Nitroimidazo[1,2-*a*]Pyridines Are NTR1 Substrates That Display Potent *in Vitro* Antileishmanial Activity. *ACS Med. Chem. Lett.* **2019**, *10*, 34–39. [CrossRef] [PubMed]

12.	Fersing, C.; Boudot, C.; Paoli-Lombardo, R.; Primas, N.; Pinault, E.; Hutter, S.; Castera-Ducros, C.; Kabri, Y.; Pedron, J.; Bourgeade-Delmas, S.; et al. Antikinetoplastid SAR Study in 3-Nitroimidazopyridine Series: Identification of a Novel Non-Genotoxic and Potent Anti-T. b. Brucei Hit-Compound with Improved Pharmacokinetic Properties. *Eur. J. Med. Chem.* **2020**, *206*, 112668. [CrossRef] [PubMed]

13.	Castera, C.; Crozet, M.D.; Vanelle, P. An efficient synthetic route to new imidazo[1,2-*a*]pyridines by cross-coupling reactions in aqueous medium. *Heterocycles* **2005**, *65*, 2979–2989. [CrossRef]